

**Journal of
Mechanics of
Materials and Structures**

**MODAL ANALYSIS OF LAMINATED BEAMS WITH FUZZY CORE
STIFFNESS/FUZZY INTERLAYER SLIP**

Rudolf Heuer and Franz Ziegler

Volume 6, No. 1-4

January–June 2011

 **mathematical sciences publishers**

MODAL ANALYSIS OF LAMINATED BEAMS WITH FUZZY CORE STIFFNESS/FUZZY INTERLAYER SLIP

RUDOLF HEUER AND FRANZ ZIEGLER

Dedicated to the memory of the late Marie-Louise and in the honor of Professor Charles R. Steele

It is mainly the matrix in composite structures that exhibits fuzzy randomness of the material parameters. When extending the work on two-layer and symmetric, three-layer viscoelastic beam, plate, and shell structures based on the definition of an equivalent effective homogeneous model, to include either fuzzy pure elastic interface slip or fuzzy core stiffness, by means of modal analysis we succeed in working out the effects on the dynamic properties of these fuzzy structures. Modal coupling by the light damping forces is neglected. Fully analyzed within the scope of this paper is a simply supported sandwich beam with fuzzy elastic core material parameters. The analysis of this illustrative example is based on the interval representation (that is, on the set of α -cuts) with a triangular membership function of the core shear stiffness prescribed. Membership functions of the undamped natural frequencies are defined using fuzzy set theory, however, avoiding artificial uncertainties. Under time-harmonic excitation, the dynamic magnification factors and, with light and deterministic modal structural damping taken into account, the fuzzy phase angles of the steady modal response are evaluated. Where appropriate, envelope functions are defined.

1. Introduction

The material of the matrix in composite lightweight structures has a large volume fraction and thus should be of low density and low cost: as a consequence of the technological processes its material parameters are less standardized when compared to high-strength fibers or reinforcing sheets. To predict the safe limits of the structural response and to account for such a variety of the structural properties a fuzzy randomness in the material parameters is prescribed. Thus generally, analyses require application of the fuzzy finite element method; see, for example, [Hanss and Willner 2000; Möller and Beer 2004]. Alternatively, for the formulation using stochastic finite elements, see, for example, [Dasgupta 2008]. When extending the work on two-layer and symmetric viscoelastic three-layer beam, plate, and shell structures based on the essential definition of an effective equivalently homogenized model, see [Adam et al. 2000; Irschik et al. 2000; Hansen et al. 2005; Heuer 2007], to include either fuzzy pure elastic interface slip (the physical interface exhibits a large variability in the material parameters differing from those of the neighboring layers) or fuzzy core stiffness (the lightweight core material is of similar consistency to a matrix material), we can avoid numerical analysis schemes and analytically work out the effects on the dynamic properties of these fuzzy thin-walled structures. Within the scope of this paper, a simply supported sandwich beam with fuzzy elastic core material parameters is fully analyzed by way of example. It should be mentioned that the solution technique remains applicable to even polygonal

Keywords: layered beams, fuzziness, interlayer slip, modal analysis, isosceles uncertainty.

composite plates since a decomposition into two “membranes” has been explored [Heuer et al. 1992; Heuer 2007].

The analysis of the illustrative example, mentioned above, is based on the interval formulation by referring to the set of α -cuts with a (triangular) membership function of the core shear stiffness prescribed. Another interpretation of such an interval number in a closed set is a random variable whose probability density function is unknown but nonzero only in the range of the interval. A recent interval dynamic modal analysis of an uncertain cantilevered shear beam with prescribed lower and upper bounds of the closed set of the shear modulus, [Modares et al. 2010], transformed the deterministic natural frequencies to their inclusive set values. Similarly, membership functions of the more complex undamped natural frequencies of the fuzzy layered beam are defined using fuzzy set theory [Zadeh 1965; Dubois and Prade 1997; Viertl and Hareter 2006], however, avoiding artificial uncertainties. Under time-harmonic excitation the problem is solved in closed form: the dynamic magnification factors and, with light modal structural damping taken into account (thereby neglecting the effects of modal coupling by the light damping forces), the fuzzy phase angles of the modal response are evaluated. Where possible, envelope functions are defined. Such modal response studies of layered beams within the interval formulation allow us to consider the worst case, by either putting the lower limit of the shear modulus of the core material to zero or by taking into account fully delaminated layers. Thus, with the deterministic assigned stiffness known, the lower branch of the membership function can be defined without the requirement of additional data. However, precision engineering may require narrowing the limits of the set of α -cuts of selected natural frequencies: the consequence on the allowable material variability (lower and upper bounds) is addressed. Subsequently, some practically important effects caused by asymmetric uncertainty of the material parameters with respect to the upper branch of the membership function are discussed. Consequently, it can be concluded that the fuzzy set of the core material provides the most appropriate model: starting with the worst-case scenario, all more restrictive bounds can be considered in an inversely taken step of rather simple additional computation without prior knowledge of material data. Since the action of imposed eigenstrains (for example, in the case of nonstationary thermal loads or in the case of piezoelectric strains in smart layers) is considered in the homogenized equivalent fuzzy beam, a fuzzy controller can be designed to annihilate the forced vibrations even under the condition of no additional stress or, relaxed, of no additional stress resultants (see [Ziegler 2005] for “impotent eigenstrains”); the definition is given by [Mura 1991]. To explore the variability of the (light) damping effects related to a fuzzy retardation time of the linear viscous model is left for future investigations since modal decomposition is crucial for the analytical results presented in this paper.

2. Linear viscoelastic layered beams

2.1. Three-layer beams. Sandwich structures are commonly defined as three-layer type constructions consisting of two thin face layers of high-strength material attached to a moderately thick core layer of low strength and density [Plantema 1966; Stamm and Witte 1974; Altenbach et al. 2004]. Dynamic response analyses require higher-order theories. A review of the equivalent single layer and layerwise laminate theories is provided by [Reddy 1993]; see also [Irschik 1993; Backström and Nilsson 2005]. The effects of interlayer slip have been discussed for elastic bonding in [Hoischen 1954; Goodman and Popov 1968; Chonan 1982], and for more general interlayer slip laws in [Murakami 1984]. In [Heuer

2004], complete analogies are presented between various models of viscoelastic sandwich structures, with or without interlayer slip, with homogenized single-layer structures of effective parameters.

Figure 1 shows the free-body diagram of a three-layer beam. Introducing the parameter

$$d = \frac{h_1 + h_2}{2} \quad (1)$$

and applying conservation of angular momentum to all three layers gives the relations

$$\begin{aligned} M_{1,x} - Q_1 - T_1 \frac{h_2}{2} - N_{1,x} d &= 0, \\ M_{2,x} - Q_2 + (T_1 + T_2) \frac{h_2}{2} &= 0, \\ M_{3,x} - Q_3 - T_2 \frac{h_2}{2} + N_{3,x} d &= 0, \end{aligned} \quad (2)$$

where T_1 and T_2 denote the interlaminar shear forces per unit length, and Q_i is the transverse shear force in the i -th layer. The bending moments M_i refer to the individual layer axes. Conservation of momentum in the axial and transverse directions renders

$$N_{1,x} + T_1 = 0, \quad N_{2,x} - T_1 + T_2 = 0, \quad N_{3,x} - T_2 = 0, \quad (3)$$

$$\sum_{i=1}^3 Q_{i,x} + p = \mu \ddot{w}, \quad \mu = \sum_{i=1}^3 \rho_i A_i. \quad (4)$$

Summation of (2) yields the global, classical conservation of momentum:

$$M_{,x} - Q = 0, \quad (5)$$

where

$$M = \sum_{i=1}^3 M_i - (N_1 - N_3) d, \quad Q = \sum_{i=1}^3 Q_i. \quad (6)$$

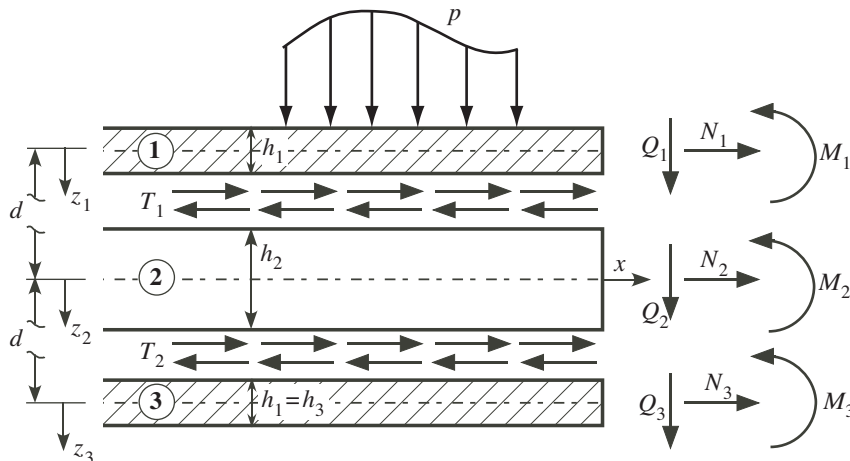


Figure 1. Geometry and stress resultants of a laterally loaded symmetric three-layer beam.

Considering the kinematic assumptions according to the first-order shear-deformation theory applied to each layer, the displacement field in the i -th layer is of the form

$$\begin{bmatrix} u_i \\ w_i \end{bmatrix} = \begin{bmatrix} u_i^{(0)} + z_i \psi_i \\ w \end{bmatrix}, \quad i = 1, 2, 3, \quad (7)$$

where $u_i^{(0)}$ and ψ_i are respectively the axial deformation and cross-sectional rotation of the i -th layer. Applying the linearized strain-displacement relations together with a linear viscoelastic constitutive law, and denoting by ϑ the retardation time of the single parameter viscous model,

$$\begin{pmatrix} \sigma_{xx}(x, z; t) \\ \tau_{xz}(x, z; t) \end{pmatrix} = \begin{pmatrix} E(z_i)[\epsilon_{xx}(x, z_i; t) + \vartheta \dot{\epsilon}_{xx}(x, z_i; t) - \epsilon_{xx}^*(x, z_i; t)] \\ G(z_i)[\gamma_{xz}(x, z_i; t) + \vartheta \dot{\gamma}_{xz}(x, z_i; t)] \end{pmatrix}, \quad (8)$$

the stress resultants of each layer are determined from

$$\begin{bmatrix} N_i \\ M_i \\ Q_i \end{bmatrix} = \begin{bmatrix} D_i & 0 & 0 \\ 0 & B_i & 0 \\ 0 & 0 & S_i \end{bmatrix} \begin{bmatrix} u_{i,x}^{(0)} + \vartheta \dot{u}_{i,x}^{(0)} - e_i^* \\ \psi_{i,x} + \vartheta \dot{\psi}_{i,x} - \kappa_i^* \\ \psi_i + w_{,x} + \vartheta (\dot{\psi}_i + \dot{w}_{,x}) \end{bmatrix}, \quad i = 1, 2, 3, \quad (9)$$

where

$$e_i^* = \frac{1}{A_i} \int_{A_i} \epsilon_{xx}^* dA, \quad \kappa_i^* = \frac{1}{J_i} \int_{A_i} \epsilon_{xx}^* z dA, \quad (10)$$

and

$$D_i = E_i A_i = E_i b h_i, \quad B_i = E_i J_i = E_i \frac{b h_i^3}{12}, \quad S_i = \kappa^2 G_i A_i = \kappa^2 G_i b h_i; \quad (11)$$

ϵ_{xx}^* , e_i^* , and κ_i^* are the imposed strain, the imposed mean strain, and the curvature (of thermal nature or resulting from electromagnetic fields applied to smart layers), respectively. The dimensions b and h_i denote a constantly assumed width and the individual layer thickness, respectively; κ^2 stands for a shear factor.

For symmetrically three-layer beams with perfect bonds the following assumptions are made:

- (1) The thin faces of high strength material are rigid in shear:

$$\begin{aligned} \psi_1 &= \psi_3 = -w_{,x}, \\ u_1^{(0)} &= u_2^{(0)} + \frac{1}{2}(h_1 w_{,x} - h_2 \psi_2), \\ u_3^{(0)} &= u_2^{(0)} - \frac{1}{2}(h_1 w_{,x} - h_2 \psi_2). \end{aligned} \quad (12)$$

- (2) The individual bending stiffness of the faces are not neglected:

$$B_i = E_i \frac{b h_i^3}{12} \neq 0, \quad i = 1, 3. \quad (13)$$

- (3) The bending stiffness of the core (its material is of low density and strength) is neglected:

$$B_2 = 0 \implies M_2 = B_2(\psi_{2,x} + \vartheta \dot{\psi}_{2,x} - \kappa_2^*) = 0. \quad (14)$$

Alternatively, for sandwich beams with viscoelastic interlayer slip [Adam et al. 2000], the classical assumption of all three layers being rigid in shear is made, with the shear traction in the physical interfaces of vanishing thickness being proportional to the displacement jumps with a viscoelastic interface stiffness understood. Hence, contrary to perfectly bonded laminates, elastic interlayer slips, Δu_1 between upper face and core and Δu_2 between lower face and core, are considered. The displacement field in the i -th layer is of the form

$$\begin{bmatrix} u_i \\ w_i \end{bmatrix} = \begin{bmatrix} u_i^{(0)} - z_i w_{,x} \\ w \end{bmatrix}, \quad i = 1, 2, 3, \quad (15)$$

where the axial deformations $u_i^{(0)}$ can be written as

$$u_1^{(0)} = u_2^{(0)} + (dw_{,x} - \Delta u_1), \quad u_3^{(0)} = u_2^{(0)} - (dw_{,x} - \Delta u_2). \quad (16)$$

The relative horizontal displacement between two layers causes linear viscoelastic shear tractions at the interfaces,

$$T_i = k(\Delta u_i + \vartheta \Delta \dot{u}_i), \quad (17)$$

where the parameter k denotes the slip modulus and

$$\Delta u_1 = dw_{,x} + u_2^{(0)} - u_1^{(0)}, \quad \Delta u_2 = dw_{,x} - u_2^{(0)} + u_3^{(0)}. \quad (18)$$

Differentiating (17) with respect to the axial coordinate x by taking into account (18) and substituting (3) and (9) renders

$$N_{1,xx} - N_{3,xx} - \frac{k}{D_1}(N_1 - N_3) + 2kd(w_{,xx} + \vartheta \dot{w}_{,xx}) - k(e_1^* - e_3^*) = 0. \quad (19)$$

Furthermore, by means of (6)₁ and (9), the difference of the axial forces can be expressed by

$$N_1 - N_3 = -\frac{1}{d}[B_0(w_{,xx} + \vartheta \dot{w}_{,xx} + \kappa^{*(0)}) + M], \quad B_0 = \sum_{i=1}^3 B_i, \quad \kappa^{*(0)} = \frac{1}{B_0} \sum_{i=1}^3 B_i \kappa_i^*. \quad (20)$$

Inserting (20) into (19) and using (4) and (5) to eliminate the bending moment M , the equation of motion takes on the desired form, namely of an exact homogenization of the viscoelastic composite beam,

$$\begin{aligned} (w_{,xxxxxx} + \vartheta \dot{w}_{,xxxxxx}) - \lambda^2(w_{,xxxx} + \vartheta \dot{w}_{,xxxx}) + \frac{\mu}{B_0} \ddot{w}_{,xx} - \lambda^2 \frac{\mu}{B_\infty} \ddot{w} \\ = -\frac{\lambda^2}{B_\infty} p + \frac{1}{B_0} p_{,xx} + \lambda^2 \kappa_{,xx}^* - \kappa_{,xxxx}^{*(0)}. \end{aligned} \quad (21)$$

In (21), p denotes the lateral load per unit of length. In smart layers, we may impose eigenstrains ϵ_x^* , for example, piezoelectric strain, for control purpose. Consequently, the eigencurvature terms have been considered in (21) for the sake of completeness in the case of nonstationary thermal loads and further

investigations of vibration control and smart piezoelectric layers,

$$\begin{aligned}\kappa^{*(0)} &= \frac{1}{B_0} \sum_{i=1}^3 \frac{12B_i}{h_i^3} \int_{h_i} \epsilon_x^* z_i dz, \\ \kappa^* &= \frac{1}{B_\infty} \left[2D_1 d \left(\frac{1}{h_3} \int_{h_3} \epsilon_x^* dz - \frac{1}{h_1} \int_{h_1} \epsilon_x^* dz \right) + \sum_{i=1}^3 \frac{12B_i}{h_i^3} \int_{h_i} \epsilon_x^* z_i dz \right].\end{aligned}\quad (22)$$

In addition, with the self-explanatory effective parameters — see Figure 1 and Equation (1) for the notation — we have

$$\begin{aligned}\mu &= 2\rho_1 h_1 + \rho_2 h_2, & D_1 &= D_3 = E_1 b h_1, & B_1 &= B_3 = E_1 \frac{b h_1^3}{12}, \\ B_0 &= B_1 + B_3, & B_\infty &= B_0 + 2D_1 d^2, & B_0/B_\infty &= [1 + 3(1 + h_2/h_1)^2]^{-1} \leq \frac{1}{4}.\end{aligned}\quad (23)$$

The shear coefficient in (21) is either proportional to the core's shear modulus G_2 in the case of perfectly bonded interfaces, i.e., (see [Heuer 2004])

$$\lambda^2 = (\kappa^2 G_2) \frac{2b}{h_2} \frac{B_\infty}{D_1 B_0},\quad (24)$$

or, for the symmetric three-layer beam with elastic interlayer slip, it becomes proportional to the elastic stiffness k when common to both physical interfaces:

$$\lambda^2 = k \frac{B_\infty}{D_1 B_0}.\quad (25)$$

Thus, (24) and (25) when substituted in (21) render qualitatively one and the same result with, for example, hard-hinged supports of a single-span beam understood.

For completeness we note also the gross bending moment and the shear force related to the deflection w and its derivatives:

$$M = -B_\infty (w_{,xx} + \vartheta \dot{w}_{,xx} + \kappa^*) + \frac{B_\infty}{\lambda^2} \left(w_{,xxxx} + \vartheta \dot{w}_{,xxxx} + \frac{\mu}{B_0} \ddot{w} + \kappa_{,xx}^{*(0)} \right), \quad Q = M_{,x}.\quad (26)$$

Since (26) contains high-order spatial derivatives, numerical calculations require further considerations: the deflection should be partitioned into its quasistatic part and the (modally expanded and truncated) complementary dynamic response. The quasistatic solution is either evaluated in exact closed form or determined by means of the method of influence functions. For details of the partitioning procedure see again [Adam et al. 2000].

2.2. Two-layer beams with interlayer slip. In the following section the governing homogenized equation (21) given above for symmetric three-layer sandwich beams is modified for asymmetric two-layer elastic beams exhibiting the important defect of viscoelastic interlayer slip. Such a model refers to the practically very important case of a single-span compound bridge consisting, for example, of a steel girder connected (elastically) to the concrete deck; for details see, for example, [Girhammar and Pan 1993]. Figure 2 shows the free body diagram of such a two-layer beam with marked centroids, S_1 and S_2 , of the individual

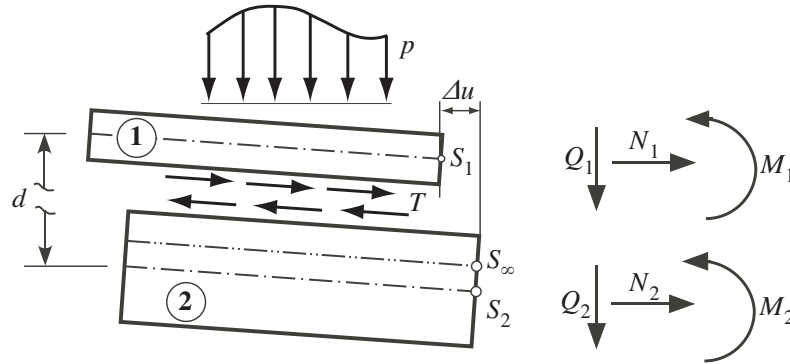


Figure 2. Geometry and stress resultants of a laterally loaded two-layer beam with linear (visco)elastic interlayer slip.

cross-sections, and, as well, global elastic center, S_∞ , of the gross composite cross-section. The partial cross-sectional areas are denoted by A_1 and A_2 ; thus, the lateral coordinate of S_∞ is determined by

$$z_\infty = \frac{D_2}{D_0}d, \quad D_0 = D_1 + D_2, \quad D_i = E_i A_i, \quad i = 1, 2. \quad (27)$$

Neglecting the effect of rotational inertia, the conservation of the angular momentum about the lateral y -axis yields the classical relationship

$$M_{,x} = Q, \quad M = M_1 + M_2 - N_1 d, \quad (28)$$

where M is the gross bending moment (see again Figure 2). In the case of no external axial forces the equilibrium condition becomes simply

$$N_1 + N_2 = 0. \quad (29)$$

Conservation of momentum in the axial direction, when applied in the free body diagram to both individual layers, gives

$$N_{1,x} = -T_1, \quad N_{2,x} = T_2, \quad (30)$$

and the continuity condition of the interfacial shear force T renders

$$T = T_1 = T_2. \quad (31)$$

T is the shear force per unit of length continuously transmitted through the interface between the two layers.

Due to the interlayer slip to be considered between the layers (see again Figure 2), the Bernoulli–Euler hypothesis is not applicable for the cross-section as a whole. However, the assumption that plane sections remain plane after deformation is still valid for either layer, respectively. Considering geometrically linearized conditions for both, the lateral and the axial deformations yield

$$w = w_1 = w_2, \quad \Delta u = u_2^{(0)} - u_1^{(0)} + dw_{,x}. \quad (32)$$

The relative horizontal displacement between the two layers causes shear tractions at the interface, where again a linear viscoelastic relation is assigned, see Equation (17),

$$T = k(\Delta u + \vartheta \Delta \dot{u}), \quad (33)$$

where k is the elastic slip modulus [Hoischen 1954; Girhammar and Pan 1993]. Differentiating (33) with respect to the axial coordinate x and substituting (29), (30), and (32)₂ lead to

$$N_{1,xx} - kN_1 \left(\frac{1}{D_1} + \frac{1}{D_2} \right) + kd(w_{,xx} + \vartheta \dot{w}_{,xx}) - k(e_1^* - e_3^*) = 0. \quad (34)$$

The axial force is expressed by means of (28)₂ with cross-sectional resultants of the constitutive relations inserted,

$$N_1 = -\frac{1}{d} [B_0(w_{,xx} + \vartheta \dot{w}_{,xx} + \kappa^{*(0)}) + M], \quad B_0 = \sum_{i=1}^2 B_i, \quad \kappa^{*(0)} = \frac{1}{B_0} \sum_{i=1}^2 B_i \kappa_i^*. \quad (35)$$

Finally, the exactly homogenized equation of motion results qualitatively in the form of (21); however the definitions (22) and (23) must be properly adapted to account for the beam with two layers — see (38) below — and essentially, this new parameter is to be substituted in (21):

$$\lambda^2 \rightarrow \lambda_2^2 = k \left(\frac{1}{D_1} + \frac{1}{D_2} + \frac{d^2}{B_0} \right). \quad (36)$$

3. The linear elastic layered beam with fuzzy stiffness

To explore the effects of fuzzy elastic material parameters and to make a modal analysis possible, the viscous effects in the homogenized equation (21) are neglected. Fuzziness of the light damping forces can be based on (21) but needs a separate investigation and thus is left for future consideration. Since no attempts are made within this paper to control the vibrations and no thermally driven vibrations are analyzed, the terms in (21) referring to imposed strains are no longer taken into account. Consequently, (21) takes on the simpler form, see also [Heuer et al. 2003], however, generalized by its explicit dependence on a fuzzy parameter,

$$w_{,xxxxxx} - \lambda^2 w_{,xxxx} + \frac{\mu}{B_0} \ddot{w}_{,xx} - \lambda^2 \frac{\mu}{B_\infty} \ddot{w} = -\frac{\lambda^2}{B_\infty} p + \frac{1}{B_0} p_{,xx}. \quad (37)$$

Thus, the shear coefficient in (37) is considered proportional to the fuzzy core shear modulus G_2 either in the case of perfectly bonded interfaces of a symmetric three-layered beam, when (24) applies, or in the practically even more important case of a two-layer beam with fuzzy elastic interface slip, with (36) substituted. In addition, the latter case requires a change in the expression of the limiting flexural stiffness given in (23); it becomes

$$B_\infty = B_0 + \frac{D_1 D_2}{D_1 + D_2} d^2. \quad (38)$$

Fuzziness in (37) is thus simply introduced by inserting, for example, a triangular membership function either for the core's shear modulus in (24) or for the physical interface stiffness in (36). Consequently the analysis of the illustrative example of a simply supported beam, as mentioned above, is based on

the interval representation, that is, the set of α -cuts. In both cases, the analysis can be based on the structurally relevant worst-case assumption of the lower bound, that is, of a maximum width of the fuzzy set by the cut at $\alpha = 0$, to include either the classical sandwich beam of vanishing core stiffness or no bond at the interface between two layers (fully delaminated), thereby avoiding the use of unreliable data on the variability of the material parameters.

Subsequently, we consider the fuzzy core stiffness of the three-layer beam in some detail.

3.1. Modal analysis of the elastic three-layer beam, hard-hinged support. For the single-span beam with hard hinged support, the homogeneous equation (37) yields the simple orthonormalized mode shapes of free vibrations:

$$\phi_n(x) = A_n \sin \beta_{1n}x, \quad \beta_{1n} = n\pi/l, \quad A_n = \left[\frac{\mu l}{2} \left(\frac{\lambda^2}{B_\infty} + \frac{\beta_{1n}^2}{B_0} \right) \right]^{-\frac{1}{2}}, \quad (39)$$

with λ^2 in that case substituted from (24).

The corresponding (undamped) circular natural frequencies are

$$\left(\frac{\omega_n(\alpha)}{\omega_{n\infty}} \right)^2 = \frac{(B_0/B_\infty) + \gamma_{2,n}k_2(\alpha)}{1 + \gamma_{2,n}k_2(\alpha)}, \quad (40)$$

when referred to

$$\omega_{n\infty}^2 = \beta_{1n}^4 B_\infty / \mu \quad (41)$$

with the fuzzy nondimensional elastic material constant of the core (typically made of a low-density, low-cost matrix material) substituted:

$$k_2(\alpha) = [\kappa_2^2 G_2(\alpha)] / (\kappa_2^2 G_2)_0. \quad (42)$$

The assigned constants are referred to the mean shear rigidity of the core (see again Figure 1):

$$(\kappa_2^2 G_2)_0 = [\kappa_2^2 G_2(\alpha = 1)], \quad \gamma_{2,n} = (\kappa_2^2 G_2)_0 \frac{2b}{\beta_{1n}^2 D_1 h_2}. \quad (43)$$

In this relation, the shear coefficient κ_2 must not be numerically specified. The monotonic behavior of the eigenfrequencies of positive-definite mechanical systems was proven by [Mullen and Modares 2009]; see (40).

The normalizing factor in (39) becomes fuzzy too. The largest level set at $\alpha = 0$ may include the worst case of a core with vanishing stiffness (or a delaminated composite). Due to the lack of reliable core material data, such a choice is recommended for the analysis. Putting constraints on the fuzziness of the dynamic parameters inversely results in a more narrow specification of the allowable largest parameter interval of the core material (see Section 4.2 for details):

$$\Delta k_{2,0} = \Delta(\kappa_2^2 G_2)_0 / (\kappa_2^2 G_2)_0 \leq 1. \quad (44)$$

The linear functions plotted in Figure 3, both intersecting at $\alpha = 1$, arise when, for the sake of simplicity, an isosceles triangular membership function is assumed:

$$\min k_2(\alpha) = 1 - \Delta k_{2,0}(1 - \alpha), \quad \max k_2(\alpha) = 1 + \Delta k_{2,0}(1 - \alpha). \quad (45)$$

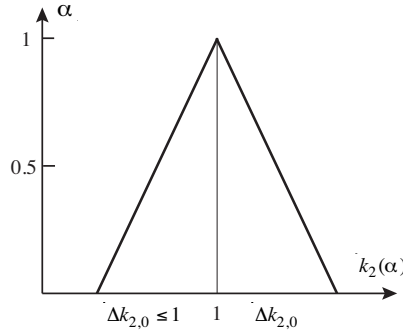


Figure 3. Three-layer beam: uncertainty of the core shear stiffness, under the assumption of an isosceles membership function.

These two equations are substituted into (40), when considering the fuzzy set in Figure 3, giving respectively the lower and upper branches of the membership functions of the natural frequencies.

Since light modal damping is commonly considered in the steady-state response of the modal oscillators to time-harmonic forcing (thus neglecting any modal coupling resulting from the viscous deformations) the dynamic magnification factor and the phase angle for every assigned forcing frequency ($\omega/\omega_{n\infty}$) become uncertain functions with the parameter α . For the sake of simplicity, constant light modal damping coefficients are assumed, $\xi = \xi_n \ll 1$, $n = 1, 2, 3, \dots$. The dynamic magnification factor can be delineated in the proper form (see, for example, [Ziegler 1998]),

$$\chi_n = \left\{ 1 - 2(1 - 2\xi^2) \left(\frac{\omega}{\omega_n(\alpha)} \right)^2 + \left(\frac{\omega}{\omega_n(\alpha)} \right)^4 \right\}^{-1/2}. \quad (46)$$

However, clearly any set of light modal damping coefficients $\zeta_1 \leq \zeta_2 \leq \dots \leq \zeta_n \leq \zeta_n + 1$ can be accounted for in (46) when estimated according to a design class of the beam.

The phase angle is given for every assigned nondimensional forcing frequency ($\omega/\omega_{n\infty}$) as a function of α , as follows (see [Ziegler 1998]):

$$\tan \phi_n = 2\xi \frac{\omega}{\omega_{n\infty}} \left[\omega_n(\alpha)/\omega_{n\infty} - \left(\frac{\omega}{\omega_{n\infty}} \right)^2 \frac{\omega_{n\infty}}{\omega_n(\alpha)} \right]^{-1}. \quad (47)$$

When (40) is substituted in (46) and (47), these equations become explicitly dependent on the fuzzy variable, (42); in particular, we get

$$\tan \phi_n = 2\xi \frac{\omega}{\omega_{n\infty}} \left[\sqrt{\frac{(B_0/B_\infty) + \gamma_{2,n} k_2(\alpha)}{1 + \gamma_{2,n} k_2(\alpha)}} - \left(\frac{\omega}{\omega_{n\infty}} \right)^2 \sqrt{\frac{1 + \gamma_{2,n} k_2(\alpha)}{(B_0/B_\infty) + \gamma_{2,n} k_2(\alpha)}} \right]^{-1}. \quad (48)$$

Again, considering the fuzzy set in Figure 3, (45) is respectively substituted in (40), (46), and (47), to yield explicitly the envelope functions of the fuzzy dynamic magnification factor and of the fuzzy phase angle as well.

4. Numerical results: fuzzy sandwich beam

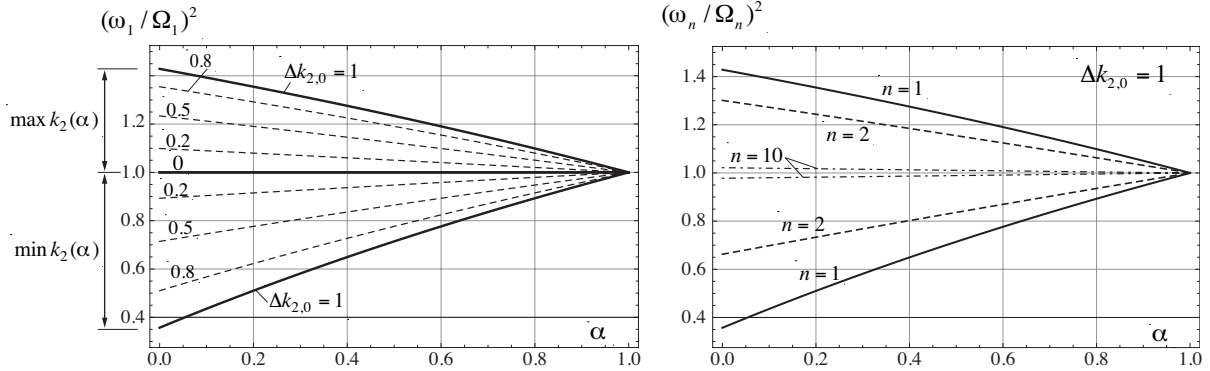


Figure 4. Three-layer beam. Left: uncertainty of the fundamental frequency ratio for various widths of fuzzy core stiffness. Right: uncertainty of the natural frequencies relative to the natural frequencies of the same order for $\alpha = 1$, for largest width of fuzzy core stiffness.

4.1. Isosceles uncertainty. (See Figure 3.) Two basic parameters are assigned for the elastic three-layer beam of Section 3, with constant light modal damping $\xi_n = \xi = 0.05$ understood throughout:

$$B_0/B_\infty = 0.1 < \frac{1}{4}, \quad \gamma_{2,n=1} = 0.25. \quad (49)$$

In the course of numerical analyses, it was found to be most illustrative to refer the frequencies to the deterministic natural circular frequencies at $\alpha = 1$. With $\Omega_n = \omega_n(1)$, Equation (40) reads

$$\left(\frac{\Omega_n}{\omega_{n\infty}}\right)^2 = \frac{(B_0/B_\infty) + \gamma_{2,n}}{1 + \gamma_{2,n}}. \quad (50)$$

This equation is evaluated first to explore the influence of the width of uncertainty on the fundamental frequency; see Figure 4, left. Considering the largest structurally possible uncertainty in the isosceles membership function of Figure 3, the intervals of uncertainty of the natural frequencies of higher order, $n \leq 10$, are depicted in Figure 4, right, relative to their values at $\alpha = 1$, (50). These membership functions become more informative when referred to the assigned fundamental frequency Ω_1 : see Figure 5.

The envelope function of the dynamic magnification factor of the basic mode, that is, putting $n = 1$ in (46), is plotted in Figure 6 varying the width of uncertainty according to Figure 3 in the $\alpha = 0.2$ cut; the forcing frequency is referred to Ω_1 . Considering maximum uncertainty (the worst-case scenario) but taking into account the whole range of parameter α gives the envelope surfaces in Figure 7. The $\alpha = 0.2$ cut yields the envelope functions of the first three modes as plotted in Figure 8.

Complementary to Figure 6, the variations of the range of uncertainty of the phase angle of the basic mode with the width of uncertainty according to Figure 3 in the $\alpha = 0.2$ cut are shown in Figure 9; the forcing frequency is again referred to the assigned fundamental frequency Ω_1 . To complement Figure 8, the ranges of uncertainty of the first three phase angles are plotted in Figure 10.

4.2. Constraints affecting the uncertain natural frequencies. Constraints on the design uncertainty, say on the uncertainty of the core shear stiffness of the three-layered beam, are often based on limiting the maximum allowable variability of the natural frequencies in a given frequency window, see [Massa

et al. 2008]. By inspection of Figure 5 it is easily recognized that such constraints can be expressed in assigning fractions of the frequency intervals (where the maximum structural width of uncertainty has been considered) that are maximum at $\alpha = 0$. Thus, a 50% reduction of that maximum result interval is chosen and, we refer to the assigned fundamental frequency Ω_1 ,

$$\frac{\omega_{n,\max}(\alpha) - \omega_{n,\min}(\alpha)}{\Omega_1} \leq [\omega_{n,\max}(\alpha = 0) - \omega_{n,\min}(\alpha = 0)]/2\Omega_1, \quad n = 1, 2, \dots, 5. \quad (51)$$

The frequency window includes and is limited by the mode number 5 for some practical reasons. Hence, the resulting α -cut is determined by solving the equation

$$\frac{\omega_{5,\max}(\alpha) - \omega_{5,\min}(\alpha)}{\Omega_1} = [\omega_{5,\max}(\alpha = 0) - \omega_{5,\min}(\alpha = 0)]/2\Omega_1. \quad (52)$$

with (45) substituted.

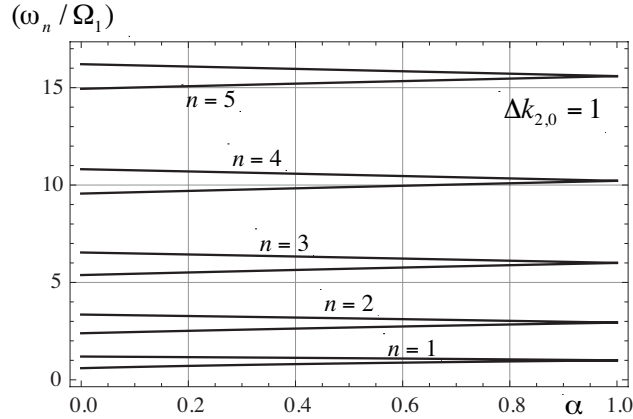


Figure 5. Three-layer beam: uncertainty of the first five natural frequencies relative to the fundamental frequency for $\alpha = 1$; increasing fuzziness observed.

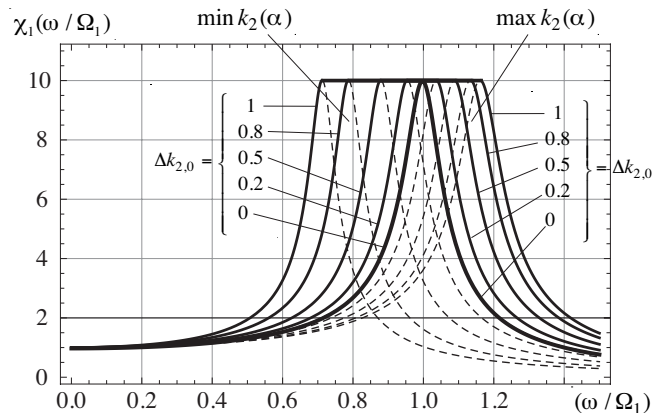


Figure 6. Three-layer beam: uncertainty of the first dynamic magnification factor for the single $\alpha = 0.2$ cut, varying the maximum interval of the fuzzy core stiffness.

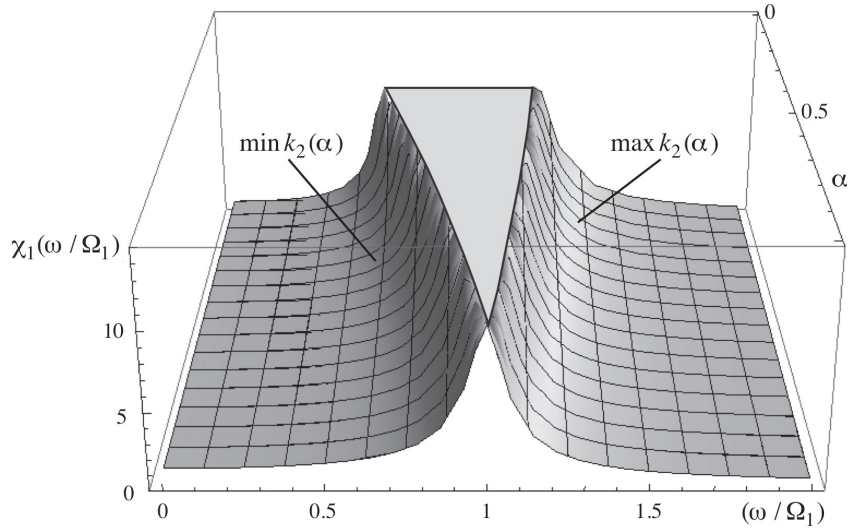


Figure 7. Three-layer beam: uncertainty surfaces of the dynamic magnification factor of the fundamental mode, light modal damping assigned.

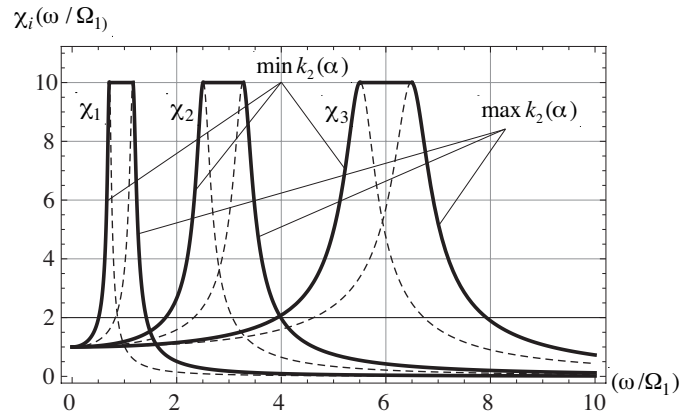


Figure 8. Three-layer beam: envelopes of the first three dynamic magnification factors for the single $\alpha = 0.2$ cut; increasing fuzziness observed.

Alternatively, it might fit the needs of precision design to limit the uncertainty relatively to the sure natural frequency of the same order of the mode (see Figure 6). We thus refer to Ω_n :

$$\frac{\omega_{n,\max}(\alpha) - \omega_{n,\min}(\alpha)}{\Omega_n} \leq [\omega_{n,\max}(\alpha = 0) - \omega_{n,\min}(\alpha = 0)]/2\Omega_n, \quad n = 1, 2, 3, \dots \quad (53)$$

In that case of relative uncertainty, the fundamental frequency interval gives the maximum tolerable uncertainty in the core shear stiffness if we solve for α the equation

$$\frac{\omega_{1,\max}(\alpha) - \omega_{1,\min}(\alpha)}{\Omega_1} = [\omega_{1,\max}(\alpha = 0) - \omega_{1,\min}(\alpha = 0)]/2\Omega_1. \quad (54)$$

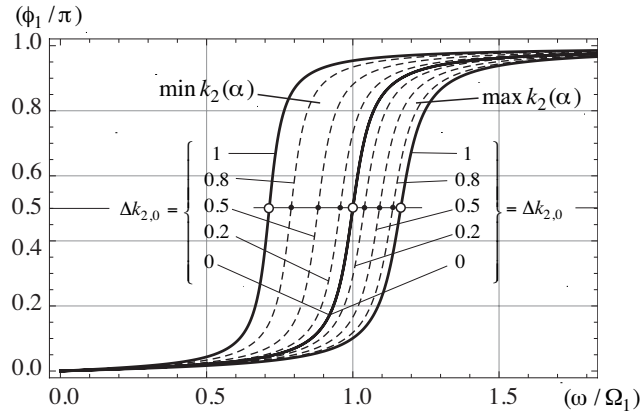


Figure 9. Three-layer beam: uncertainty of the first phase angle for the single $\alpha = 0.2$ cut, maximum interval of the fuzzy core stiffness varied; complement of Figure 6.

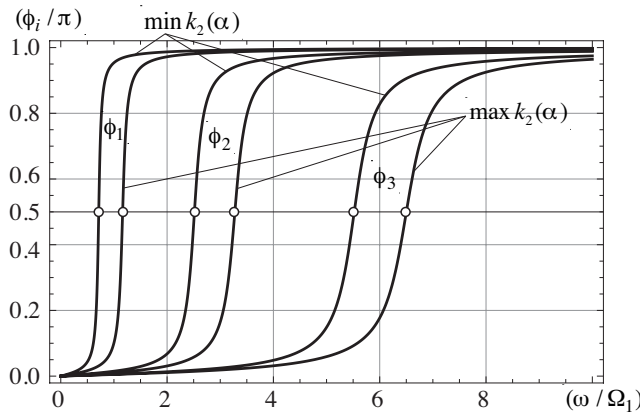


Figure 10. Three-layer beam: the envelopes of three phase angles for the single $\alpha = 0.2$ cut; complementing Figure 8; increasing fuzziness observed.

Since the largest width of uncertainty of the core shear stiffness is considered in Figures 5 and 6, the constraints allow the definition of the allowable α -cuts by solving either (52), to render $\alpha(n = 5) \doteq 0.50$, or alternatively, (54), to yield the less stringent condition at $\alpha(n = 1) \doteq 0.44$. The maximum bases of the allowable isosceles membership functions of the uncertainty of the core shear stiffness in the more precise designs are plotted in Figure 11.

4.3. Some effects of nonsymmetric uncertainty. We consider the extreme (worst) case of $\Delta k_{2,0} = 1$, that is, (45) when generalized reduces to $\min k_2(\alpha) = \alpha$, $\max k_2(\alpha) = 1 + \Lambda(1 - \alpha)$, where $\Lambda > 1$ renders the maximum core stiffness enlarged in Figure 3. The extremes of upper and lower bounds of

the neighboring natural frequencies thus are obtained for the $\alpha = 0$ cut, (42) is properly adapted,

$$\begin{aligned} \max \left(\frac{\omega_n}{\omega_{n,\infty}} \right)_{\alpha=0}^2 &= \frac{(B_0/B_\infty) + \gamma_{2,1}(1 + \Lambda)/n^2}{1 + \gamma_{2,1}(1 + \Lambda)/n^2}, & \omega_{n,\infty}^2 &= n^4 \beta_{1,1}^4 (B_\infty/\mu), \\ \min \left(\frac{\omega_{n+1}}{\omega_{n+1,\infty}} \right)_{\alpha=0}^2 &= (B_0/B_\infty) \leq 1/4, & \omega_{n+1,\infty}^2 &= (n+1)^4 \beta_{1,1}^4 (B_\infty/\mu). \end{aligned} \quad (55)$$

A first effect of asymmetric uncertainty in an ensemble of fuzzy beams is observed by putting $\max \omega_n^2 = \min \omega_{n+1}^2$ rendering the coefficient of asymmetry,

$$\Lambda = \Lambda(n) = \frac{(B_0/B_\infty)}{\gamma_{2,1}} \frac{n^2 \left[\left(\frac{n+1}{n} \right)^4 - 1 \right]}{\left[1 - (B_0/B_\infty) \left(\frac{n+1}{n} \right)^4 \right]} - 1 > 0. \quad (56)$$

The parameters assumed in Section 4.1, $(B_0/B_\infty) = 0.1$ and $\gamma_{2,1} = 0.25$, exclude a solution of (56) for $n = 1$ and yield the coefficients of asymmetry: $\Lambda(n = 2) = 12.16$, $\Lambda(n = 3) = 10.37$, $\Lambda(n = 4) = 11.20$, $\Lambda(n = 5) = 12.54$, $\Lambda(n = 6) = 14.07$, $\Lambda(n = 7) = 15.68$, ... Equation (56), when virtually considered for continuous order n exhibits a singularity at $n = 1.28$. It is moved to $n = 1$ for the smaller ratio of the flexural stiffness $B_0/B_\infty = 1/16 \approx 0.063$. Since $\max B_0/B_\infty = 0.25$, reported in (23), the singularity at $n = 2$ is still possible for the flexural stiffness ratio $B_0/B_\infty = 0.198$, but no effect on higher modes is observed for $n \geq 3$. Consequently, for these two ratios of the flexural stiffness, a violation of the assumption of a triangular membership function of uncertainty is observed and consequently the solution for the coefficient of asymmetry becomes invalid.

5. Conclusions

For symmetric three-layer slender beam, thin plate and thin shell structures, and for a two-layer composite an exact homogenization exists, which is worked out in detail for the hard hinged supported

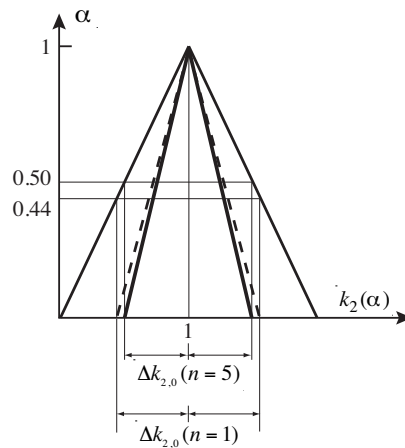


Figure 11. Three-layer beam: reduction of the intervals of uncertainty under the conditions of 50% constraints of either uncertainty of the first five natural frequency intervals, $n = 5$, or of the relative natural frequency intervals, $n = 1$.

beam. Consequently, interval mathematics becomes applicable to the solution of the sixth-order resulting homogenized equation with a fuzzy parameter either of a fuzzy core shear stiffness and/or fuzzy stiffness of the physical interface between layers to define the intervals of the dynamic response. A detailed study of a three-layer simply hard supported beam with fuzzy core of an isosceles membership function is performed, giving lower and upper bounds of the natural frequencies and providing deep insights into level-sets of the dynamic magnification factors and of the phase angles in forced time harmonic vibrations. Fuzziness of dynamic parameters like natural frequencies, dynamic magnification factors, and modal phase angles increases with frequency as expressed by the modal order. This efficient analysis can be performed without reliable knowledge of the uncertainty of the material parameters by considering structurally inherent worst-case scenarios. It yields exact and robust results, preserves the problem's physics, and obtaining bounds does not require expensive stochastic procedures such as Monte Carlo simulations. Putting constraints on the variability, say of the natural frequencies, leads to the maximum tolerable uncertainty in the core shear stiffness and/or that of the stiffness of the physical interface. Effects within an ensemble of such beams, for example, overlapping of the intervals of their natural frequencies, however, under the assumption of a nonsymmetric triangular membership function of the core stiffness uncertainty, are shown to be limited to the first and second modes. Either fuzzy modal superposition or fuzzy control of vibrations can be based on the results of this paper. However, since the normalizing factor of the orthogonal mode shapes turns out to be fuzzy too, the complexity of modal superposition is increased. Thus, modal superposition of forced vibrations becomes fuzzy in both time records and amplitude response. Superposition of the modal maxima by considering the square root of sum of squares yields the (approximate) total displacement response even in this more complex case. The analysis of a fuzzy retardation time of viscoelastic layers (such a fuzzy parameter is included in the homogenized equation) leads to coupled modal equations even in a Ritz–Galerkin approximation and is out of the scope of this paper. It is left to future investigations.

6. Acknowledgement

This research has been supported by a Hochschuljubiläumfonds der Stadt Wien research grant provided by the city of Vienna. The authors are indebted to the two anonymous reviewers for their constructive criticism and fruitful comments. Discussions on the relevant parts of the interval formulation with Professor Reinhard Viertl, TU Vienna, are gratefully acknowledged.

References

- [Adam et al. 2000] C. Adam, R. Heuer, A. Raue, and F. Ziegler, “Thermally induced vibrations of composite beams with interlayer slip”, *J. Therm. Stresses* **23**:8 (2000), 747–772.
- [Altenbach et al. 2004] H. Altenbach, J. Altenbach, and W. Kissing, *Mechanics of composite structural elements*, Springer, Berlin, 2004.
- [Backström and Nilsson 2005] D. Backström and A. Nilsson, “Flexural vibrations of a three-layer sandwich beam: using ordinary fourth order beam theory in combination with frequency dependent parameters to predict the flexural dynamics of a sandwich beam”, pp. 567–576 in *Sandwich structures 7: advancing with sandwich structures and materials* (Aalborg, 2005), edited by O. T. Thomsen et al., Springer, Dordrecht, 2005. Part 5.
- [Chonan 1982] S. Chonan, “Vibration and stability of sandwich beams with elastic bonding”, *J. Sound Vib.* **85**:4 (1982), 525–537.

- [Dasgupta 2008] G. Dasgupta, “Stochastic shape functions and stochastic strain-displacement matrix for a stochastic finite element stiffness matrix”, *Acta Mech.* **195** (2008), 379–395.
- [Dubois and Prade 1997] D. Dubois and H. Prade, “The three semantics of fuzzy sets”, *Fuzzy Sets Syst.* **90**:2 (1997), 141–150.
- [Girhammar and Pan 1993] U. A. Girhammar and D. Pan, “Dynamic analysis of composite members with interlayer slip”, *Int. J. Solids Struct.* **30**:6 (1993), 797–823.
- [Goodman and Popov 1968] J. R. Goodman and E. P. Popov, “Layered beam systems with interlayer slip”, *J. Struct. Div. (ASCE)* **94** (1968), 2535–2547.
- [Hansen et al. 2005] J. S. Hansen, G. Kennedy, and S. F. M. de Almeida, “A homogenization based theory for laminated and sandwich beams”, pp. 221–230 in *Sandwich structures 7: advancing with sandwich structures and materials* (Aalborg, 2005), edited by O. T. Thomsen et al., Springer, Dordrecht, 2005. Part 3.
- [Hanss and Willner 2000] M. Hanss and K. Willner, “A fuzzy arithmetical approach to the solution of finite element problems with uncertain parameters”, *Mech. Res. Commun.* **27**:3 (2000), 257–272.
- [Heuer 2004] R. Heuer, “Equivalence of the analyses of sandwich beams with or without interlayer slip”, *Mech. Adv. Mater. Struct.* **11**:4–5 (2004), 425–432.
- [Heuer 2007] R. Heuer, “Equivalences in the analysis of thermally induced vibrations of sandwich structures”, *J. Therm. Stresses* **30**:6 (2007), 605–621.
- [Heuer et al. 1992] R. Heuer, H. Irschik, and F. Ziegler, “Thermally forced vibrations of moderately thick polygonal plates”, *J. Therm. Stresses* **15**:2 (1992), 203–210.
- [Heuer et al. 2003] R. Heuer, C. Adam, and F. Ziegler, “Sandwich panels with interlayer slip subjected to thermal loads”, *J. Therm. Stresses* **26**:11–12 (2003), 1185–1192.
- [Hoischen 1954] A. Hoischen, “Verbundträger mit elastischer und unterbrochener Verdübelung”, *Bauingenieur* **29** (1954), 241–244.
- [Irschik 1993] H. Irschik, “On vibrations of layered beams and plates”, *Z. Angew. Math. Mech.* **73**:4-5 (1993), T34–T45.
- [Irschik et al. 2000] H. Irschik, R. Heuer, and F. Ziegler, “Statics and dynamics of simply supported polygonal Reissner–Mindlin plates by analogy”, *Arch. Appl. Mech.* **70**:4 (2000), 231–244.
- [Massa et al. 2008] F. Massa, K. Ruffin, T. Tison, and B. Lallemand, “A complete method for efficient fuzzy modal analysis”, *J. Sound Vib.* **309**:1–2 (2008), 63–85.
- [Modares et al. 2010] M. Modares, I. Olabarri, and R. L. Mullen, “Reliable dynamic analysis of an uncertain shear beam”, pp. 173–185 in *REC 2010: proceedings of the 4th International Workshop on Reliable Engineering Computing* (Singapore, 2010), edited by M. Beer et al., Research Publication Service, Singapore, 2010.
- [Möller and Beer 2004] B. Möller and M. Beer, *Fuzzy randomness*, Springer, Berlin, 2004.
- [Mullen and Modares 2009] R. L. Mullen and M. Modares, “Free vibration of structures with interval uncertainty”, in *Proceedings of the 9th ASCE Speciality Conference on Probabilistic Mechanics and Structural Reliability (PMC2004)* (Albuquerque, NM, 2004), Curran, Red Hook, NY, 2009.
- [Mura 1991] T. Mura, *Micromechanics of defects in solids*, 2nd ed., Kluwer, Dordrecht, 1991.
- [Murakami 1984] H. Murakami, “A laminated beam theory with interlayer slip”, *J. Appl. Mech. (ASME)* **51**:3 (1984), 551–559.
- [Plantema 1966] F. J. Plantema, *Sandwich construction*, Wiley, New York, 1966.
- [Reddy 1993] J. N. Reddy, “An evaluation of equivalent-single-layer and layerwise theories of composite laminates”, *Compos. Struct.* **25** (1993), 21–35.
- [Stamm and Witte 1974] K. Stamm and H. Witte, *Sandwichkonstruktionen*, Springer, New York, 1974.
- [Viertl and Hareter 2006] R. Viertl and D. Hareter, *Beschreibung und Analyse unscharfer Information: Statistische Methoden für unscharfe Daten*, Springer, Berlin, 2006.
- [Zadeh 1965] L. A. Zadeh, “Fuzzy sets”, *Information and control* **8** (1965), 338–353.
- [Ziegler 1998] F. Ziegler, *Mechanics of solids and fluids*, 2nd corrected ed., Springer, New York, 1998.
- [Ziegler 2005] F. Ziegler, “Computational aspects of structural shape control”, *Comp. Struct.* **83**:15–16 (2005), 1191–1204.

Received 18 Mar 2010. Revised 21 Jun 2010. Accepted 6 Jul 2010.

RUDOLF HEUER: rudolf.heuer@tuwien.ac.at

Civil Engineering Department, Vienna University of Technology, Karlsplatz 13/E2063, A-1040 Vienna, Austria

FRANZ ZIEGLER: franz.ziegler@tuwien.ac.at

Civil Engineering Department, Vienna University of Technology, Karlsplatz 13/E2063, A-1040 Vienna, Austria